

Geometry and bonding in alkali-metal-atom–antimony ($A_n\text{Sb}_4$) clusters

F. Hagelberg, S. Neeser, N. Sahoo, and T. P. Das

Department of Physics, State University of New York at Albany, Albany, New York 12222

K. G. Weil

Department of Materials Science and Engineering, The Pennsylvania State University, University Park, Pennsylvania 16802

(Received 27 December 1993)

The structures and stabilities of $A_2\text{Sb}_4$, $A_4\text{Sb}_4$, and $A_6\text{Sb}_4$ clusters ($A=\text{Li, Na, K, and Cs}$), some of which were detected by Knudsen effusion mass spectrometry, are investigated in this work by Hartree-Fock pseudopotential optimization. For each system examined, we consider two structural alternatives: one involving a tetrahedral Sb_4 cluster nucleus and another containing a square of four Sb atoms. The high electronegativity differences between antimony and alkali-metal-atom cluster constituents give rise to a sizable electron transfer from the alkali-metal atoms to the Sb_4 unit, which tends to flatten out the Sb_4 tetrahedron. From our calculations, the systems $A_2\text{Sb}_4$ and $A_4\text{Sb}_4$ appear to be highly polar compounds consisting of a symmetric arrangement of alkali-metal atoms above and below an Sb_4 square. For $A_6\text{Sb}_4$ complexes, in contrast, no unique characterization can be given. While an Sb_4 square variant is proposed for $A_6\text{Sb}_4$ clusters with $A=\text{Na, K, and Cs}$, for the Li_6Sb_4 cluster a structure that contains a tetrahedral Sb_4 unit is more likely. In general, all the $A_n\text{Sb}_4$ clusters studied here exhibit substantial polarity. The Cs_6Sb_4 system, however, is characterized by metallic bonding features.

PACS number(s): 36.40.+d, 31.20.-d, 35.20.Bm, 35.20.Dp

I. INTRODUCTION

The recent interest in the physics and chemistry of antimony atom clusters (Sb_n) is largely motivated by the complex binding features observed in bulk antimony. Here, metallic bonding coexists with molecular or covalent structures [1,2], so that antimony clusters are expected to exhibit a range of different bonding types.

As has been demonstrated by electronic time-of-flight mass spectroscopy [3], tetramer packings of antimony atoms, i.e., units of the form Sb_{4n} , are characterized by an especially high stability. Evaporation of solid antimony yields mainly Sb_4 particles [4]. By Hartree-Fock investigation, the structure of this cluster was examined from first principles [5]. As is plausible from a comparison with the well-known structure of the group-V systems P_4 [6] and As_4 [7], the tetrahedral geometry turned out to be the actual one. Several planar structures, however, were found to be stable as well, although with lesser binding energy than the regular tetrahedron. In view of the high stability of the Sb_4 unit, it is to be expected that this complex will be found as a constituent of clusters occurring in the vapor over alkali-metal-atom–antimony compounds like solid and fused Cs_3Sb [8]. This was verified by Scheuring and Weil [9] who investigated the vapor over NaSb, KSb, and CsSb mixtures in continuation of experiments done by Neubert *et al.* [10] on the gas phase above LiSb compounds. In these studies, cluster species existing in the vapor above solid and liquid alkali-metal-atom–antimony mixtures were detected using the method of Knudsen effusion mass spectrometry. This procedure allows for both the identification of a particular species and the determination of its ionization potential [9]. In addition to these observations, studies of

ionization efficiency curves were carried out that made possible a distinction between primary products of the evaporation process and secondary products resulting from fragmentation due to electron impact. As parent species containing the Sb_4 unit, the systems Na_2Sb_4 , Na_6Sb_4 , K_2Sb_4 , K_4Sb_4 , Cs_2Sb_4 , and Cs_6Sb_4 could be isolated. These clusters can be subdivided into the groups $A_2\text{Sb}_4$, $A_4\text{Sb}_4$, and $A_6\text{Sb}_4$ with $A=\text{Na, K, and Cs}$. Obviously, the members of those groups that have been actually detected are relatively few. No unit of the form Na_4Sb_4 has been found in the NaSb vapor whereas the clusters Na_2Sb_4 and Na_6Sb_4 both occur, having approximately equal abundances [9]. In the KSb vapor both a K_2Sb_4 and a K_6Sb_4 cluster seem to be lacking. Finally, the mass spectrometric experiments carried out so far do not indicate the presence of a Cs_4Sb_4 cluster in the CsSb vapor. No $A_n\text{Sb}_4$ units have been detected in the LiSb vapor [10]. The existence of smaller series of the form Li_nSb_m ($m < 4$), however, has been reported by Neubert *et al.* [10].

For reasons of technical practicability, the experiments have been so far restricted to the alkali-metal-atom species Li, Na, K, and Cs; no data on RbSb or FrSb mixtures are available at present. The *ab initio* investigations presented in this work, which aim at a comparison with results of measurements, will focus exclusively on antimony in combination with the alkali elements Li, Na, K, Cs for which experimental data are available.

The reported results raise the question if, from the point of view of quantum chemistry, the systems not yet isolated are unstable, or if they are stable in principle, and some further experimental effort could lead to their discovery in the future. Moreover, one could ask how the clusters found stable by *ab initio* investigation com-

pare with respect to their stabilization energies, the latter quantities in each case representing the difference between the total electronic energy of the cluster at equilibrium geometry and the sum of the energies of the cluster constituents at infinite separation. From the variations of this quantity, characteristic differences between stabilities of individual cluster systems can be inferred.

Any understanding of features related to the stability of clusters requires the knowledge of their structures. From experiment, nothing is known so far about the geometry of the alkali-metal-atom-antimony compounds discussed here. In this work, we want to propose structures of these clusters that appear to be the most likely ones from energy minimization using the Hartree-Fock procedure. In a first approach to the structure problem, one might assume a regular arrangement of alkali-metal atoms grouped around a tetrahedral Sb_4 cluster nucleus. However, as a result of the generally large electronegativity differences between antimony and alkali-metal atoms [11], a sizable electron transfer from the alkali-metal atom to the antimony constituents of the clusters will occur which can lead to a distortion of the Sb_4 tetrahedron as is explained in further detail in Sec. III. Depending on the polarity of the alkali-metal-atom-antimony bonding realized in the cluster, tetrahedral or planar geometry of the Sb_4 is possible. The analysis described in the following sections aims at a detailed examination of this structural alternative.

Besides considerations pertaining to structure and geometry, the most crucial question in the physics and chemistry of $A_n\text{Sb}_4$ systems is: How does the nature of bonding change with the number of alkali-metal-atom constituents? We will try to characterize the bonding in the systems that this study concentrates on by a comparison of electron transfer from the alkali-metal atom to the antimony atoms in different clusters.

Section II of this paper contains an outline of the procedure followed in this work. Our results will be presented and discussed in Sec. III. Section IV adds some concluding remarks.

II. PROCEDURE

In this work, investigations on three different cluster groups are presented, namely, $A_2\text{Sb}_4$, $A_4\text{Sb}_4$, and $A_6\text{Sb}_4$ with $A = \text{Li, Na, K, and Cs}$. For each of these systems, two Hartree-Fock geometry optimizations were carried out, one involving a structure that contains a square arrangement of Sb atoms, and another one in which the Sb_4 nucleus has the regular tetrahedral form. Motivations for our special choices of cluster geometries are given in Sec. III. For each individual system, the minimal energy was determined as a function of geometrical parameters using the Fletcher-Powell optimization method [12].

For each system, a geometry optimization using the pseudopotential procedure applied on a Gaussian minimal basis set [13–15] was employed in a preliminary step. The variational coefficients and geometrical parameters resulting from this treatment were subsequently reused as the initial choices of a more comprehensive calculation. In this second step, a Gaussian double zeta

basis set [13–15] was employed, supplemented by polarization functions [16] that were of p character for the alkali-metal-atom constituents and of d character for the Sb atoms under examination.

The pseudopotential approach applied here is necessitated by the large sizes of some of the systems which are the subject of this research, like Cs_6Sb_4 . For this and for other clusters under consideration, an all-electron analysis would be prohibitively extensive. In order to achieve methodological consistency, we use the same approach also in the investigation of smaller systems like Li_2Sb_4 or Na_2Sb_4 . For the clusters containing lithium atoms, however, the assumption of an inert alkali-metal-atom ion core cannot be maintained, since there is a sizable overlap between the lithium $1s$ orbitals and the antimony valence electron states. Thus, all three electrons of the lithium shell were included in the Hartree-Fock calculations reported here. For some systems, comparison is made between nearest neighbor distances as they occur in alkali-metal-atom-antimony clusters, and molecular bond lengths of the species A_2^+ , A_3^+ , and alkali-Sb-metal-atom. This study was motivated by the question for the bonding type realized in the examined systems. If the small molecules mentioned above can be identified as substructures of the more complex $A_n\text{Sb}_4$ clusters one has to conclude that polar bonding strongly dominates in the investigated compounds. All systems were treated in exactly the same way, i.e., the same double zeta basis sets and polarization functions were used in the evaluation of equilibrium bond lengths for the smaller molecules as for the $A_n\text{Sb}_4$ compounds.

We have tested the reliability of our procedure involving pseudopotentials and a polarized Gaussian double zeta basis set by carrying out a structure optimization for the Sb_4 molecule. A global energy minimum was found for a regular tetrahedron of four Sb atoms with an Sb—Sb bond length of $R = 2.84 \text{ \AA}$. This agrees very well with the value reported by Zhang and Balasubramanian [17] who obtained an Sb_4 bond length of $R = 2.874 \text{ \AA}$. Their calculation was based on a complete active space multiconfiguration procedure followed by multireference configuration interaction (CASMCF-MRCI) where up to two million configurations were included. The work of Zhang and Balasubramanian represents the most comprehensive quantum-chemical treatment of the Sb_4 unit done so far.

We also find good agreement with the result of a Hartree-Fock all-electron geometry optimization where a Gaussian minimal basis set was used [5]. This procedure yielded $R = 2.80 \text{ \AA}$. It should be noted that a pseudopotential geometry optimization [5] in which minimal basis functions were employed instead of the polarized double zeta basis set used in the present work led to a value of $R = 3.05 \text{ \AA}$. This finding considerably overestimates the Sb—Sb bond length of Sb_4 , and with our present choice of basis functions we obtain a clearly more realistic result.

In the special case of the cluster Na_6Sb_4 , our treatment yielded a near degeneracy of the Sb_4 square variant and the Sb_4 tetrahedron variant of this system (see Sec. III).

For a more reliable comparison of the stabilities of the two possible cluster structures, electron correlation had to be taken into account. Thus we improved on the results achieved by application of the Hartree-Fock method by carrying out a refined calculation based on the configuration interaction technique [18]. Since we are dealing throughout with closed-shell systems, only determinants with double substitutions were included, in keeping with the Brillouin theorem. All investigations described here were performed using the program GAUSSIAN 92 and the IBM RISC 6000 cluster system at the Cornell National Supercomputer Facility.

The main aspects of comparison for the individual cluster systems discussed in the following are stability and electron transfer from the alkali-metal-atom constituents to the Sb_4 nucleus of the cluster. We obtained stabilization energies using the formula

$$\Delta E_{\text{stab}} = \sum_{i=1}^n E_{\infty}(A_i) + 4E_{\infty}(\text{Sb}) - E(A_n\text{Sb}_4),$$

n = number of alkali atoms contained in the cluster ,

A_i = i th alkali-metal atom of the cluster .

The quantity E_{∞} refers to the energy of the respective cluster constituent at infinite separation from any other elements and $E(A_n\text{Sb}_4)$ denotes the total energy of the cluster at equilibrium. By "electron transfer" we mean the net charge concentrated on the Sb_4 cluster nucleus at equilibrium geometry. This value is found from a Mulliken population analysis [19] of the molecular orbitals determined by Hartree-Fock investigation.

III. RESULTS AND DISCUSSION

The geometry of the free Sb_4 cluster is tetrahedral. As has been shown by arguments based on the Jahn-Teller theorem [5], the square arrangement of four Sb atoms is unstable. This structure, however, is stabilized when two electrons are added to the Sb_4 complex. In a preliminary investigation, we compared the stabilities of a tetrahedral and a square variant of the Sb_4^{2-} species. For both clusters, bond length optimizations were carried out using the polarized double zeta pseudopotential basis set [13–15] mentioned in Sec. II. For the Sb_4^{2-} tetrahedron, we find an Sb—Sb equilibrium bond length of $R(\text{Sb—Sb}) = 3.04 \text{ \AA}$, corresponding to a minimal energy of $E = -567.5 \text{ eV}$. In the square variant of the Sb_4^{2-} cluster, the bond length shrinks to $R(\text{Sb—Sb}) = 2.77 \text{ \AA}$, and the minimal energy is lowered by 3.2 eV. In conclusion, the double-negatively charged Sb_4 system clearly prefers the square structure over the tetrahedral one, whereas the neutral system exhibits stability in tetrahedral, but not in square, geometry. Another conceivable way of stabilization of an Sb_4 square unit consists in the addition of alkali-metal atoms that can act as electron donors to the Sb_4 nucleus. In the following, we discuss the three groups of $A_n\text{Sb}_4$ clusters investigated experimentally so far: $A_2\text{Sb}_4$, $A_4\text{Sb}_4$, and $A_6\text{Sb}_4$. For each system, we examine both variants mentioned above, one containing the Sb_4 nucleus as a regular tetrahedron and another one in which the Sb_4 square structure is realized.

A. Clusters of the form $A_2\text{Sb}_4$

For $A_2\text{Sb}_4$ clusters, symmetry considerations suggest a square arrangement of four Sb atoms with one alkali-metal atom above and one below their plane as a likely structure [see Fig. 2(a)]. This idea is supported by an investigation of the highest occupied electronic levels of the $A_2\text{Sb}_4$ system. Figure 1 shows the corresponding level scheme as compared to the highest occupied levels of the Sb_4 square system, both schemes referring to the spin singlet configuration. The two degenerate E_g orbitals of the pure Sb_4 square cluster are only partially filled, indicating the occurrence of the pseudo-Jahn–Teller effect [20] and consequently the instability of this structure. In the case of the $A_2\text{Sb}_4$ cluster, in contrast, these levels are completely occupied so that no Jahn-Teller distortion will occur. Thus, addition of two alkali-metal atoms has a stabilizing effect on the Sb_4 square system in spin singlet configuration. It must be pointed out, however, that there is also another structure of $A_2\text{Sb}_4$ complexes conceivable that would preserve the regular tetrahedral geometry of the free Sb_4 unit. The $A_2\text{Sb}_4$ cluster could consist of an A_2 dumbbell piercing through an Sb_4 tetrahedron. A highly symmetric structure that realizes this geometry is the one illustrated by Fig. 2(b). The two alkali-metal atoms are located on a plane that intersects the midpoint of an Sb—Sb edge at a right angle, and contains the centroid of the Sb_4 tetrahedron. The lines joining the centroid to the two alkali-metal atoms have equal length and subtend angle α , as shown in Fig. 2(b). From the symmetry characters of the highest occupied orbitals, as shown in Fig. 1(b), this structure is expected to be stable, too. Table I lists the result of a comparative study of both possible $A_2\text{Sb}_4$ structures with $A = \text{Li, Na, K}$,

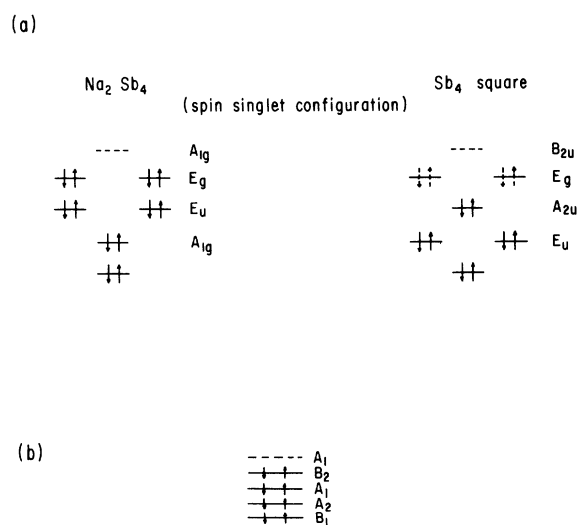


FIG. 1. (a) Comparison of level schemes for the higher occupied states of $A_2\text{Sb}_4$ (square) and Sb_4 (square); the broken arrows represent the partially filled characters of the highest occupied levels. (b) Level scheme of the highest occupied states for the tetrahedral variant of $A_2\text{Sb}_4$.

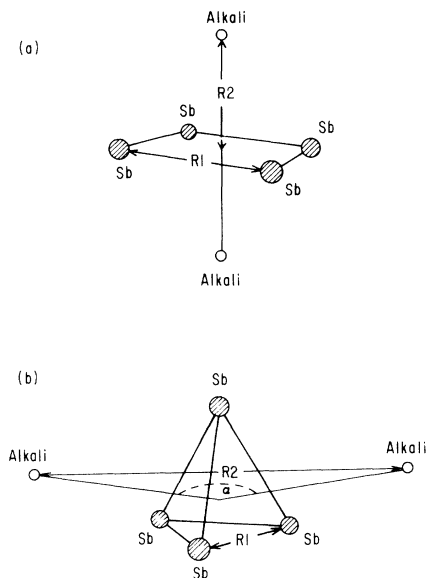


FIG. 2. (a) A_2Sb_4 (square) and (b) A_2Sb_4 (tetrahedron) geometries. The geometrical optimization parameters R_1 , R_2 , and α , as explained in the text, are indicated.

and Cs. Optimized bond lengths are given along with stabilization energies from Hartree-Fock calculation and with effective charges of the Sb_4 cluster nuclei obtained from Mulliken population analysis [18]. As is obvious from a comparison of the stabilization energies of the two examined structures, the clusters that contain Sb_4 in square geometry consistently turn out to be lower in energy than those involving a tetrahedral Sb_4 unit. The proposed square geometry is therefore the stabler one and more likely to occur in nature than a structure that preserves the original Sb_4 tetrahedron. The charge transfer from the alkali-metal-atom constituents to the cluster nucleus is markedly stronger in case of the Sb_4 square species than for the tetrahedral variant of the cluster. As our examination of the pure Sb_4 cluster demonstrates, addition of charge is needed to flatten out the Sb_4 unit while charge neutrality of this unit makes the tetrahedral geometry more favorable.

According to our results, the Sb_4 square variant of A_2Sb_4 is thus preferred over the Sb_4 tetrahedron variant. To examine if this finding is dependent on the pseudopotential approach and choice of basis set used in the

present work, we carried out an additional calculation on a particular system, K_2Sb_4 , including all the electrons in this cluster. We evaluated the total energies of the system for both structural alternatives at the equilibrium geometries which resulted from the preceding pseudopotential optimization. We used a polarized all-electron split valence shell basis set of composition (433321/43321/43) for the Sb constituents and (43321/43) for the K constituents of the cluster [16]. This choice of basis functions yields a total energy of $E = -718,726.25$ keV for the tetrahedral variant of K_2Sb_4 and $E = -718,728.69$ keV for the square variant. The resulting energy difference of $\Delta E = 2.44$ eV between both geometrical variants is well compatible with the pseudopotential result of $\Delta E = 2.60$ eV (see Table I). Both all-electron and pseudopotential treatments thus lead to comparable higher energies for the Sb_4 tetrahedron variant of the A_2Sb_4 cluster considered than for the Sb_4 square variant.

The stablest complex presented in Table I is the Cs_2Sb_4 cluster in square geometry. Since the high electronegativity difference between Sb and the alkali-metal atoms in question rises markedly from Na to Cs (while slightly dropping as one goes from Li to Na) [11], the charge transfer from the Cs atoms to the Sb_4 nucleus is more efficient in the case of Cs_2Sb_4 than for the remaining A_2Sb_4 clusters. The experimentally observed high abundance of Cs_2Sb_4 as compared to other A_2Sb_4 species supports our finding that the stability of this cluster is highest in the A_2Sb_4 cluster series investigated here.

Caution is advised in the interpretation of the stabilization energies for clusters containing Li (see Sec. II). In the case of Li all electrons are treated as active electrons whereas a pseudopotential approach has been used for $A = Na, K$, and Cs, and therefore the values given for the stabilization energies in Table I are quantitatively more meaningful to compare for the latter three alkali-metal-atom species.

The optimized values of the geometrical parameters for the Sb_4 square variant of the A_2Sb_4 cluster are listed in Table I(a). Their overall tendencies can be understood in terms of the individual alkali-metal-atom-Sb and alkali-metal-atom-alkali-metal-atom bonds. (Table IV gives a compilation of optimized bond lengths and stabilization energies for molecules of the form alkali-metal-atom-Sb as well as A_2^+ , where $A = Li, Na, K$, and Cs.) The in-

TABLE I. Hartree-Fock optimization results for A_2Sb_4 clusters ($A = Li, Na, K, Cs$).

System	Geometrical parameters			Minimal energy (eV)	Stabilization energy (eV)	Net charge on Sb_4 nucleus	Net charge per alkali-metal atom
	R_1 (Å)	R_2 (Å)	α				
(a) Sb_4 square arrangement							
Li_2Sb_4	2.80	2.08		-980.57	-12.84	-0.65	0.33
Na_2Sb_4	2.79	2.62		-584.96	-11.67	-1.02	0.51
K_2Sb_4	2.78	3.14		-583.36	-11.94	-1.44	0.72
Cs_2Sb_4	2.77	3.53		-582.33	-14.47	-1.59	0.80
(b) Sb_4 tetrahedral arrangement							
Li_2Sb_4	2.93	7.92	174.24	-977.68	-9.95	-0.51	0.25
Na_2Sb_4	2.90	8.70	174.10	-582.71	-9.43	-0.43	0.21
K_2Sb_4	2.88	9.63	168.37	-580.76	-9.36	-0.46	0.23
Cs_2Sb_4	2.87	10.35	161.72	-579.66	-11.55	-0.37	0.18

creasing trend of the equilibrium bond lengths of the A_2^+ molecules studied is reflected by a steady increase of the parameter R_2 in Fig. 2(a) from Li_2Sb_4 to Cs_2Sb_4 . This parameter measures the vertical distance of the alkali-metal-atom constituent from the Sb_4 plane. The equilibrium distances found for the alkali-metal-atom-Sb bond in Table IV show the same rising tendency, except for a slight contraction as one goes from SbK to SbCs .

The parameter R_1 in Fig. 2(a) refers to the bond length between two adjacent Sb atoms in the Sb_4 square unit. A small but steady decrease of this quantity from Li_2Sb_4 to Cs_2Sb_4 indicates a tightening of the Sb—Sb bond due to a gradual enhancement of charge transfer from the alkali-metal-atom to the Sb constituents of the cluster.

Electron transfer stabilizes Sb_4 in square geometry whereas the tetrahedral Sb_4 exhibits a different behavior. For the tetrahedral variants the system Cs_2Sb_4 again displays the highest stability found in the series. From Table I(b), however, one notices that the highest cluster stability here corresponds to the smallest net charge on the Sb_4 nucleus. The polarity of the system is clearly reduced as one goes from K_2Sb_4 to Cs_2Sb_4 . The Na_2Sb_4 complex appears to be slightly less polar than K_2Sb_4 and exhibits a somewhat higher stability as compared to that of the latter system. These findings are plausible in view of the destabilizing effect of electron transfer to the Sb_4 tetrahedron as discussed earlier in this section. Generally, the negative charge transferred to the Sb_4 cluster nucleus turns out to be much smaller for the tetrahedral than for the square variant of the $A_2\text{Sb}_4$ cluster. This is consistent with the much larger alkali-metal-atom-Sb bond distances that we find in the tetrahedral as compared to the square variant.

B. Clusters of the form $A_4\text{Sb}_4$

For this more complex group of $A_n\text{Sb}_4$ clusters, we again compare two possible geometries along the lines of the discussion given for the group with $n=2$. If Sb_4 square geometry is assumed, one expects to find two alkali-metal atoms each above and below the Sb_4 plane as the most likely cluster structure [see Fig. 2(a)] for $n=2$. This hypothesis is supported by the fact that A_2^+ is a stable molecule. Thus, the mechanism that stabilizes $A_2\text{Sb}_4$ in square geometry could be operative in the case

of $A_4\text{Sb}_4$ too, since the alkali-metal-atom constituents could provide the charge necessary to flatten out the Sb_4 tetrahedron. The proposed structure is therefore $A_2^+-\text{Sb}_4^{2-}$ (square)- A_2^+ . In carrying out energy optimizations for this possible structure of $A_4\text{Sb}_4$ clusters with $A = \text{Li}, \text{Na}, \text{K},$ and Cs , we used the geometrical parameters indicated in Fig. 3(a).

Table II(a) gives the results of these calculations. The stability of the $A_4\text{Sb}_4$ clusters in the Sb_4 square configuration is expected not only to be determined by the strength of charge transfer from alkali-metal-atom to Sb cluster elements but also by the strength of the interalkali-metal-atom bonds involved. As is seen from the compilation of stabilization energies quoted in Table II(a), the cluster Cs_4Sb_4 exhibits a markedly higher stability than any other $A_4\text{Sb}_4$ cluster listed. This feature is explained by the charge transfer which is higher for Cs_4Sb_4 than for the remaining compounds, and, additionally, by the strength of the Cs_2^+ bond, exceeding the bond stabilization energies of the other A_2^+ species examined in this work (compare Table IV). In fact, the distance between two Cs atoms located above or below the Sb_4 plane, which is found to be 5.76 Å, appears to be very close to the equilibrium bond length $R(\text{Cs}_2^+) = 5.85$ Å of the Cs_2^+ ion. In the K_4Sb_4 cluster, for comparison, we observe a distance between two neighboring K atoms of 5.28 Å which is significantly larger than the K_2^+ equilibrium bond length of $R(\text{K}_2^+) = 4.85$ Å. Therefore, the Cs_4Sb_4 cluster in Sb_4 square configuration seems to be closest to a realization of the tentative $A_2^+-\text{Sb}_4^{2-}$ (square)- A_2^+ structure.

The structure displayed in Fig. 3(b) can be conceived as a possible $A_4\text{Sb}_4$ geometry that preserves the tetrahedral form of the free Sb_4 cluster. In this model, four alkali-metal atoms are situated on lines that intersect the faces of a regular tetrahedron perpendicularly at their centers. The resulting structure realizes the most compact geometrical arrangement possible. It can be seen from Table II(b) that all species with this structure investigated here turn out to be stable. The equilibrium structures obtained, however, are higher in minimal energy than their counterparts that contain the Sb_4 unit in square form. This finding is plausible in view of the consistently large electron charge transfer to the Sb_4 tetrahedron which

TABLE II. Hartree-Fock optimization results for $A_4\text{Sb}_4$ clusters ($A = \text{Li}, \text{Na}, \text{K}, \text{Cs}$).

System	Geometrical parameters			Minimal	Stabilization	Net charge on	Net charge per
	R_1 (Å)	R_2 (Å)	α	energy (eV)	energy (eV)	Sb_4 nucleus	alkali-metal atom
(a) Sb_4 square arrangement							
Li_4Sb_4	2.96	2.99	88.77	-1386.16	-14.14	-1.71	0.43
Na_4Sb_4	2.96	3.44	87.12	-594.85	-11.75	-1.89	0.47
K_4Sb_4	2.95	3.90	85.21	-590.75	-11.39	-2.55	0.64
Cs_4Sb_4	2.95	4.30	84.11	-587.90	-15.13	-2.59	0.65
(b) Sb_4 tetrahedral arrangement							
Li_4Sb_4	3.31	2.75		-1383.19	-11.16	-1.60	0.40
Na_4Sb_4	3.39	3.18		-591.70	-8.59	-2.06	0.52
K_4Sb_4	3.30	3.65		-587.71	-8.35	-2.70	0.67
Cs_4Sb_4	3.04	4.26		-585.57	-12.80	-1.77	0.44

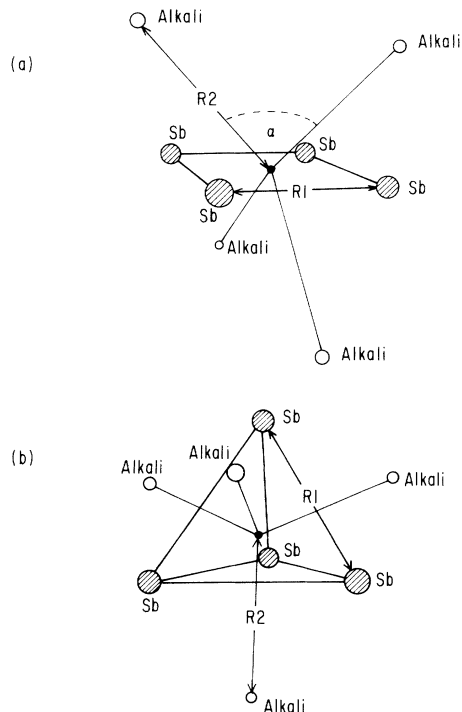


FIG. 3. (a) $A_4\text{Sb}_4$ (square) geometry. The geometrical optimization parameters R_1 , R_2 , and α are indicated, α referring to the opening angle between the two lines that connect the two upper (lower) alkali-metal atoms with the center of the Sb_4 square. (b) $A_4\text{Sb}_4$ (tetrahedron) geometry. The geometrical parameter R_1 refers to the Sb—Sb bond length while R_2 denotes the distance of the alkali-metal atoms from the center of the Sb_4 tetrahedron.

tends to destabilize it while the comparably large charge transfer to the Sb_4 square has a stabilizing effect on this structure.

The polarity of the $A_n\text{Sb}_4$ (tetrahedron) complex increases continuously as one goes from $A = \text{Li}$ to $A = \text{K}$, accompanied by a steady decrease of the stabilization energy of the cluster. A sizably smaller net charge is found on the Sb_4 nucleus of the Cs_4Sb_4 (tetrahedron) system than on the Sb_4 nuclei of the three lighter units. This feature is reflected by a strong enhancement of the stabilization energy of the Cs_4Sb_4 (tetrahedron) cluster over the respective values of the other members of this series. The conclusion that electron addition to the Sb_4 tetrahedron reduces the cluster stability seems to be well confirmed in the case of the $A_4\text{Sb}_4$ group.

C. Clusters of the form $A_6\text{Sb}_4$

Turning to the third group of $A_n\text{Sb}_4$ clusters investigated in this work, we observe a number of new features. Guided by the findings of our examination of the $A_4\text{Sb}_4$ series, where two molecular substructures of the form A_2^+ above and below an Sb_4 square turned out to provide a highly stable geometry, we propose for $A_6\text{Sb}_4$ (square) complexes the structure $A_3^+ - \text{Sb}_4^{2-}$ (square)- A_3^+ . Similar to $A_4\text{Sb}_4$, the structure can be viewed as a combination of two stable singly charged A_m ($m = n/2$)

molecules, in the case discussed here A_3^+ ions, and an Sb_4 square stabilized by electron transfer from the two A_m units. Figure 4(a) shows the geometry that was assumed in the energy minimization calculations for the $A_6\text{Sb}_4$ clusters, also the optimization parameters are indicated.

The geometry chosen for an examination of the tetrahedral variant of the same cluster series is displayed in Fig. 4(b). The tetrahedral Sb_4 nucleus is enclosed in a regular A_6 octahedron, the six alkali-metal atoms being situated on lines that intersect the centers of the tetrahedron edges at right angles. This highly symmetric geometry realizes the most compact arrangement of the atoms possible.

A compilation of the equilibrium values obtained for the geometrical parameters used in the energy minimization of the structures introduced is presented in Table III(a) along with the minimal energies obtained and stabilization energies. The latter are mostly larger than those found for the $A_2\text{Sb}_4$ and $A_4\text{Sb}_4$ groups, which can be attributed to the enhanced number of alkali-metal-atom constituents and to the stabilizing role of their mutual interactions in the $A_6\text{Sb}_4$ species.

While for both the $A_2\text{Sb}_4$ and the $A_4\text{Sb}_4$ series, the Sb_4 square turned out to be energetically favored over the Sb_4

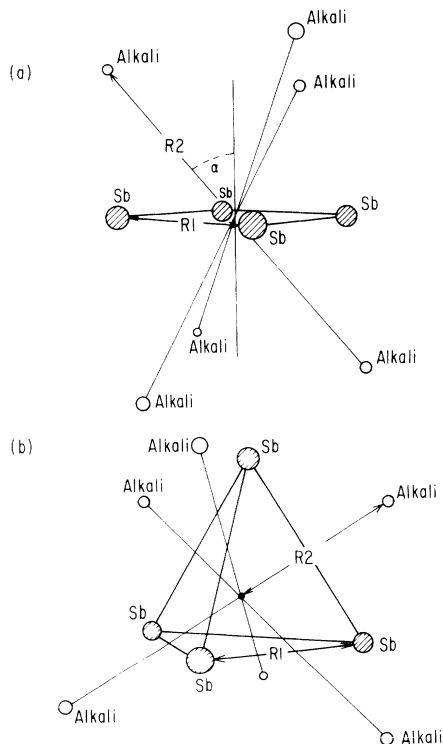


FIG. 4. (a) $A_6\text{Sb}_4$ (square) geometry. R_1 denotes the Sb—Sb bond length, R_2 stands for the distance of an alkali-metal atom from the center of the Sb_4 square. Each line connecting the center of the Sb_4 square with an alkali-metal atom includes the angle α with the middle axis. (b) $A_6\text{Sb}_4$ (tetrahedron) geometry. The geometrical parameter R_1 refers to the Sb—Sb bond length while R_2 denotes the distance of the alkali-metal atoms from the center of the Sb_4 tetrahedron.

TABLE III. Hartree-Fock optimization for A_6Sb_4 clusters ($A = Li, Na, K, Cs$).

System	Geometrical parameters		Minimal energy (eV)	Stabilization energy (eV)	Net charge on Sb_4 nucleus	Net charge per alkali-metal atom	
	R_1 (Å)	R_2 (Å)	α				
(a) Sb_4 square arrangement							
Li_6Sb_4	2.93	3.17	36.86	-1790.84	-14.54	-1.68	0.28
Na_6Sb_4	2.92	3.72	39.61	-603.68	-16.48	-2.19	0.36
$Na_6Sb_4^a$	2.92	3.72	39.61	-616.20	-29.0	-2.19	0.36
K_6Sb_4	2.95	4.18	39.79	-598.80	-11.49	-2.49	0.41
Cs_6Sb_4	2.76	4.95	37.01	-596.02	-18.59	-1.47	0.24
(b) Sb_4 tetrahedral arrangement							
Li_6Sb_4	3.90	3.21		-1791.47	-15.15	-2.59	0.43
Na_6Sb_4	4.45	3.62		-603.64	-16.46	-2.83	0.47
$Na_6Sb_4^a$	4.45	3.62		-615.28	-28.1	-2.83	0.47
K_6Sb_4	5.51	4.07		-596.62	-9.33	-3.54	0.59
Cs_6Sb_4	6.71	4.38		-592.10	-14.66	-3.39	0.56
(c) Differences in stabilization energies between tetrahedral and square variant of A_6Sb_4 clusters, $\Delta E_{stab} = E_{stab}(Sb_4 \text{ square variant}) - E_{stab}(Sb_4 \text{ tetrahedral variant})$.							
System	ΔE_{stab} (eV)						
Li_6Sb_4	-0.61						
Na_6Sb_4	0.02						
$Na_6Sb_4^*$	0.90						
K_6Sb_4	2.16						
Cs_6Sb_4	3.93						

^aResults of configuration interaction calculations at equilibrium geometry as found from Hartree-Fock investigation.

tetrahedron variant for all alkali-metal atoms, this structure does not seem to be realized consistently in A_6Sb_4 clusters. As is obvious from the results listed in Table III, minimal and stabilization energies of the Li_6Sb_4 unit come out lower for the tetrahedral than for the square variant of this cluster. For Na_6Sb_4 , the difference in minimal energies between the two structural alternatives is extremely small, amounting to less than 0.03 eV. The clusters K_6Sb_4 and Cs_6Sb_4 , in contrast, exhibit an unambiguously lower minimal energy for the square than for the tetrahedral variant.

In the following paragraphs, we want to comment first on the A_6Sb_4 (square) series and then on the tetrahedral variants of the same clusters. The Na_6Sb_4 and the K_6Sb_4 units seem to be closest to the $A_3^+ - Sb_4^{2-} - A_3^+$ structure proposed for the Sb_4 square series. An analysis of the A_3^+ units contained in the clusters Na_6Sb_4 and K_6Sb_4 reveals that their interatomic distances are close to those of the free triangular A_3^+ molecule. As the values quoted in Table IV demonstrate, the Na—Na (K—K) bond lengths in the Na_6Sb_4 (K_6Sb_4) cluster differ from the bond lengths found for the isolated Na_3^+ (K_3^+) molecule only by 1.7% (1.6%).

This feature does not carry over to the Cs_6Sb_4 cluster which seems to be stabilized by a bonding mechanism quite different from the one operative in the other A_6Sb_4 compounds. The Cs—Cs bond length of the Cs_3^+ molecule as a substructure of the Cs_6Sb_4 is reduced by 8.5% as compared to the bond length of the free Cs_3^+ species (see the data given in Table IV). One also notices a very siz-

able drop in the electron transfer as one goes from K_6Sb_4 to Cs_6Sb_4 . Whereas the clusters of the form A_2Sb_4 (Sb_4 square) and A_4Sb_4 (Sb_4 square) show an increase of electron transfer with increasing electronegativity difference between antimony and the alkali-metal-atom species in question, this behavior is found in the A_6Sb_4 (Sb_4 square) clusters only for $A = Li, Na, \text{ and } K$. We interpret this reduction of charge on the Sb_4 cluster nucleus for Cs_6Sb_4 as a result of a change in the cluster bonding characteristics. The mutual interactions of the alkali-metal atoms appear to contribute to the bonding more strongly in the Cs_6Sb_4 (Sb_4 square) cluster than in the other species of the A_6Sb_4 (Sb_4 square) group examined here.

Investigation of the molecular orbitals that our calculation yields for the Cs_6Sb_4 (Sb_4 square) complex confirms that they are composed of either purely antimony or cesium states; the coupling of antimony and alkali-metal-atom constituents is found to be much weaker here than in any other cluster explored in the context of the present work. Thus, the Cs_6Sb_4 (Sb_4 square) unit can be understood as a square arrangement of four Sb atoms surrounded by two Cs trimers. In view of the markedly diminished electron transfer to the Sb_4 cluster nucleus and the correspondingly low charge per alkali-metal-atom constituent, the Cs_6Sb_4 cluster appears to be the least polar of the systems examined here. The nature of its bonding is more properly described as metallic than as ionic. This conjecture gains support from a calculation of the ionization energy E_{ion} for this cluster. The result is $E_{ion}[Cs_6Sb_4 (Sb_4 \text{ square})] = 3.05$ (eV) which is distinctly

TABLE IV. Equilibrium bond lengths for the systems A_2^+ , A_3^+ , and A -Sb from Hartree-Fock energy minimization ($A = \text{Li, Na, K, Cs}$). For A_3^+ , the structure of an equilateral triangle is assumed. Also, stabilization energies are given that refer to the A_2^+ and the A_3^+ species. D in $A_4\text{Sb}_4$ (square) [$A_6\text{Sb}_4$ (square)] denotes the nearest neighbor bond length between two alkali-metal-atom constituents in $A_4\text{Sb}_4$ (square) [$A_6\text{Sb}_4$ (square)].

System	Optimized bond length D (Å)	D in $A_4\text{Sb}_4$ (square)	Stabilization energy (eV)
Li_2^+	3.172	4.203	1.226
Na_2^+	4.243	4.741	0.683
K_2^+	4.899	5.298	0.709
Cs_2^+	5.849	5.758	1.697
		D in $A_6\text{Sb}_4$ (square)	
Li_3^+	3.082	3.290	1.965
Na_3^+	4.179	4.108	0.869
K_3^+	4.709	4.635	0.955
Cs_3^+	5.642	5.159	2.921
LiSb	2.639		
NaSb	2.989		
KSb	3.428		
CsSb	3.396		

lower than the ionization energy we obtain for the Sb_4 square variant of the Cs_2Sb_4 cluster: $E_{\text{ion}}[\text{Cs}_2\text{Sb}_4 (\text{Sb}_4 \text{ square})] = 3.87 \text{ eV}$, indicating a more polar bonding in the latter case. The experimental findings: $E_{\text{ion}}(\text{Cs}_6\text{Sb}_4) = 3.9(0.3)$ and $E_{\text{ion}}(\text{Cs}_2\text{Sb}_4) = 4.4(0.3)$ [21] are somewhat higher than the calculated results but exhibit the same trend. The stability of the Cs_6Sb_4 (Sb_4 square) system turns out to be significantly higher than that of the other species of the group under examination.

From our findings, it appears that the cluster K_6Sb_4 is the least stable member of this group. This result offers an explanation for the fact that in Knudsen effusion mass spectrometry measurements [9], the species Na_6Sb_4 and Cs_6Sb_4 have been detected in contrast to K_6Sb_4 which has not been isolated so far.

As a characteristic feature of the tetrahedral variant we find a strongly pronounced dependence of the Sb—Sb bond length on the alkali-metal-atom cluster component. It can be seen from Table III(b) that this bond length increases steadily from 3.90 Å in Li_6Sb_4 to 6.71 Å in Cs_6Sb_4 . The strong impact of the alkali-metal-atom species on the size of the Sb_4 tetrahedron is plausible in view of the geometry chosen: The alkali-metal atoms are positioned on a line that intersects the Sb—Sb edges midway. As is to be expected, the bond between two Sb constituents is strongly affected by the presence of an alkali-metal atom located close to the midpoint of the Sb—Sb distance. This arrangement results in a weakening of the Sb—Sb bond of the Sb_4 tetrahedron leading to the observed sizable increase of the corresponding bond length over its equilibrium value which is $R_1 \approx 2.9 \text{ Å}$ [17].

As in the two $A_n\text{Sb}_4$ series discussed before, we state a relation between the electron transfer to the Sb_4 tetrahedron and the cluster stability. The net charge on the Sb_4 nucleus rises markedly as one goes from Li_6Sb_4 to K_6Sb_4 (tetrahedron), corresponding to an equally pronounced

drop in stabilization energy. The reduction of net charge on the Sb_4 tetrahedron in Cs_6Sb_4 as compared to K_6Sb_4 (tetrahedron) is accompanied by an increase in stability.

The difference in stabilization energies between the tetrahedral and the square variants of the $A_6\text{Sb}_4$ cluster increases steadily from $A = \text{Li}$ to $A = \text{Cs}$ [see Table III(b)]. For Li_6Sb_4 , the tetrahedral Sb_4 geometry appears to be favored over the square geometry. No unambiguous decision about the structure of the Na_6Sb_4 cluster could be made using the Hartree-Fock method as outlined in Sec. II since both variants under examination were separated by only $\Delta E = 0.025 \text{ eV}$. For clarification, we have carried out further calculations on the Na_6Sb_4 cluster in both possible structures taking into account valence electron correlation by the use of the configuration interaction method. Here, the wave functions that resulted from the preceding Hartree-Fock treatment of the Na_6Sb_4 system served as initial choices. The results of these two additional calculations are also given in Table III(b). From this more extended analysis, the square variant of the Na_6Sb_4 cluster is seen to be clearly lower in energy than the tetrahedral variant. The value obtained for the energy difference between both structures, $\Delta E = 0.9 \text{ (eV)}$, however, is still sizably smaller than the corresponding energy differences found for the heavier clusters of the $A_6\text{Sb}_4$ series.

For K_6Sb_4 and Cs_6Sb_4 , the Sb_4 square geometry is apparently the preferred one. The high amounts of net charge concentrated on the Sb_4 tetrahedron in both cases, correlated with an extreme stretching of the Sb—Sb bond lengths, indicate a marked destabilization of the tetrahedral Sb_4 nucleus for both clusters.

From our *ab initio* analysis of $A_n\text{Sb}_4$ ($n = 2, 4, 6$; $A = \text{Li, Na, K, Cs}$) systems, the following main observations emerge:

- (1) The Jahn-Teller instability of an Sb_4 square arrange-

ment is removed when n alkali-metal atoms are added to the Sb_4 nucleus which act as electron donors.

(2) For $n = 2$ or $n = 4$, the energetically preferred structure of $A_n\text{Sb}_4$ is associated with a square geometry (D_{4h} symmetry). In the case $n = 6$, however, the tetrahedral Sb_4 structure (T_d symmetry) exhibits a slightly smaller minimal energy than the square one for $A = \text{Li}$. The Sb_4 tetrahedron and Sb_4 square variants of the Na_6Sb_4 cluster are of similar stability. For $A = \text{K}$, Cs , in contrast, the $A_6\text{Sb}_4$ (square) clusters come out lower in minimal energy than the $A_6\text{Sb}_4$ (tetrahedron) clusters by several electron volts. This result is attributed to destabilization of the Sb_4 tetrahedron as a consequence of strong electron transfer from the alkali-metal-atom constituents to the Sb_4 nucleus.

It should be mentioned that the semiempirical one-electron extended Hückel approach used by H. Lies, M. C. Böhm, and K. G. Weil [22] leads to the same conclusion as here. The authors investigated the systems $A_n\text{Sb}_4$ ($n = 2, 4, 6$) with $A = \text{Na}$, K , and Cs in several geometries and found also a clear preference for the square planar as opposed to the tetrahedral Sb_4 structure. Both methods, the extended Hückel procedure used by Lies, Böhm, and Weil as well as the pseudopotential Hartree-Fock formalism employed in the present work yield a sizable electron transfer giving rise to the observed transition of the Sb_4 cluster nucleus from T_d to D_{4h} symmetry.

(3) The alkali-metal atoms tend to arrange themselves in ionic substructures of the form A_2^+ for $n = 4$ and A_3^+ for $n = 3$ above and below the Sb_4 square, the positive charges reflecting the generally high polarities of the systems investigated. In the case of Cs_6Sb_4 unit, however, we observe a marked reduction of the net charge on the Sb_4 nucleus. This feature is ascribed to a different type of bonding realized in the Cs_6Sb_4 (square) system as compared to the $A_6\text{Sb}_4$ (square) clusters with lighter alkali-metal atoms. The mutual interaction of the alkali-metal-atom species plays a more important role in the stabilization of the Cs_6Sb_4 unit than the alkali-metal-atom-antimony bonding, and Cs_6Sb_4 might be properly described as a metallic cluster.

(4) Within a series specified by a fixed number of alkali-metal atoms, the stability of the $A_n\text{Sb}_4$ (tetrahedron) units is widely governed by the electron transfer from the alkali-metal-atom species to the Sb_4 nucleus. Addition of electrons tends to weaken the $\text{Sb}-\text{Sb}$ bonds and to diminish the stability of the whole cluster.

IV. CONCLUSION

It has been demonstrated by total energy minimization based on the Hartree-Fock method that clusters of the form $A_n\text{Sb}_4$ with $n = 2, 4, 6$ and $A = \text{Li}$, Na , K , Cs are stable. Two equilibrium structures have been investigated, the first making allowance for a distortion of the Sb_4 tetrahedron into a square, the second preserving the tetrahedral geometry of the free Sb_4 unit. For $n = 2$ and 4, minimal energies were found consistently to be higher

in the latter than in the former case, reflecting a higher stability of $A_n\text{Sb}_4$ that contain the Sb_4 unit as a square as compared to those in which a tetrahedral arrangement is realized. This is plausible considering the strong electron transfer from the alkali-metal-atom to the antimony constituents which is characteristic for the clusters under examination due to the large electronegativity differences between antimony and alkali-metal atoms. The electron transfer to the Sb_4 cluster nucleus tends to flatten out the Sb_4 tetrahedron and to stabilize the Sb_4 square structure. The systematics of the Sb_4 variants of the $A_2\text{Sb}_4$ clusters are well understandable in terms of alkali-metal-atom-antimony electronegativity differences and the associated charge transfer from alkali-metal-atom cluster elements to the Sb_4 nucleus. From the $\text{Na}-\text{Sb}$ to the $\text{Cs}-\text{Sb}$ bond, the electronegativity difference increases, and correspondingly, increasing stability of the Sb_4 square unit and of the cluster as a whole is observed.

In the Sb_4 square variants of the $A_n\text{Sb}_4$ clusters with $n = 4, 6$, a similar correlation between alkali-metal-atom-antimony electronegativity difference and the charge transfer on the Sb_4 cluster nucleus is clearly noticeable. The stability of these complexes, however, depends sensitively on the mutual interactions of the alkali-metal-atom constituents. They tend to arrange themselves in ionic units of the form A_2^+ in $A_4\text{Sb}_4$ and A_3^+ in $A_6\text{Sb}_4$ clusters. The species Cs_6Sb_4 , however, deviates from the predominantly polar bond character of the clusters under investigation. As is signified by a strong reduction of charge transfer from alkali-metal-atom to antimony cluster components, and by the corresponding weakening of the alkali-metal-atom-antimony bonds, this complex might be regarded as an Sb_4 nucleus surrounded by a quasimetallic shell consisting of six Cs atoms.

For $n = 6$ and $A = \text{Li}$ or Na , the $A_6\text{Sb}_4$ (tetrahedron) cluster seems to be of higher or comparable stability as the $A_6\text{Sb}_4$ (square) clusters. In all other cases, the most compact geometry, involving a Sb_4 tetrahedron and a linear or a regularly tetrahedral or octahedral arrangement of alkali-metal atoms around it has turned out to be the energetically less favored of the two structural variants compared, in spite of its high degree of symmetry. This is attributed to the sizable electron transfer to the Sb_4 tetrahedron which tends to diminish its stability.

As has been shown, the stabilities of the $A_6\text{Sb}_4$ (tetrahedron) variants depend sensitively on the net charge concentrated on the tetrahedral Sb_4 nucleus. Within a certain $A_n\text{Sb}_4$ series, addition of net charge to this unit due to electron transfer from the alkali-metal-atom constituents has a destabilizing effect on the cluster as a whole.

As a consequence of our investigation, all $A_n\text{Sb}_4$ ($A = \text{Li}$, Na , K , Cs and $n = 2, 4, 6$) should in principle be detectable although with different abundances varying in accordance with the different stabilities of the cluster species.

The demonstrated fact that clusters of the form $A_6\text{Sb}_4$ exhibit high stabilities leads naturally to the question how many alkali-metal atoms an Sb_4 nucleus can maximally

accommodate. A straightforward continuation of the work presented here will be the investigation of $A_{2m}Sb_4$ clusters, $m \geq 4$, where the alkali-metal atoms are situated on the corners of regular m polygons above and below the Sb_4 square. It will be of particular interest to explore the change of bonding features as $n = 2m$ increases. Qualitatively, one expects a rise in metallicity of the cluster, as it is already noticeable in the bonding characteristics of the Cs_6Sb_4 system as compared to Cs_4Sb_4 or Cs_2Sb_4 .

Also, a continuation of our comparison between Sb_4 square and Sb_4 tetrahedron variants of the A_nSb_4 system for $n > 6$ will answer one of the main questions arising from this work: Are clusters with tetrahedral Sb_4 geometry energetically favored in case of larger numbers

of alkali-metal-atom constituents? Additional refined mass spectrometric efforts on A_nSb_4 clusters would be very valuable for an examination of the predictions made in this work. Thus, our calculations imply the existence of highly stable Na_4Sb_4 and Cs_4Sb_4 clusters not experimentally observed so far. Secondly, it would be desirable to explore if the species Li_nSb_4 ($n = 2, 4, 6$) can be detected, since they have been found to be stable from our calculations.

ACKNOWLEDGMENTS

Discussions with H. Lies and M. C. Böhm on their extended Hückel calculations are gratefully acknowledged.

-
- [1] D. Rayane, P. Melinon, B. Cabaud, A. Horeau, B. Tribollet, and M. Broyer, *Z. Phys. D* **12**, 217 (1989).
- [2] D. Rayane, P. Melinon, B. Tribollet, B. Cabaud, A. Horeau, and M. Broyer, *J. Chem. Phys.* **91**, 3100 (1989).
- [3] K. Sattler, J. Muhlbach, P. Pfau, and E. Recknagel, *Phys. Lett.* **87A**, 418 (1982).
- [4] J. Muhlbach, P. Pfau, E. Recknagel, and K. Sattler, *Surf. Sci.* **106**, 18 (1981).
- [5] F. Hagelberg, N. Sahoo, T. P. Das, K. G. Weil, and K. H. Speidel, *Phys. Rev. A* **46**, 6087 (1992).
- [6] R. R. Hart, M. B. Brown, and N. A. Kubler, *J. Chem. Phys.* **42**, 3631 (1964).
- [7] Y. Morino, T. Ukaji, and I. Ito, *Bull. Chem. Soc. Jpn.* **39**, 64 (1966).
- [8] B. Busse and K. G. Weil, *Ber. Bunsenges. Phys. Chem.* **86**, 93 (1982).
- [9] T. Scheuring and K. G. Weil, *Surf. Sci.* **156**, 457 (1985).
- [10] A. Neubert, K. F. Zmbov, K. A. Gingerich, and H. R. Ihle, *J. Chem. Phys.* **77**, 5218 (1982).
- [11] See, for instance, J. Moore, *Physical Chemistry* (Prentice-Hall, Englewood Cliffs, NJ, 1962), p. 545.
- [12] R. Fletcher and M. J. D. Powell, *Comput. J.* **6**, 163 (1963).
- [13] P. J. Hay and W. R. Wadt, *J. Chem. Phys.* **82**, 270 (1985).
- [14] W. R. Wadt and P. J. Hay, *J. Chem. Phys.* **82**, 284 (1985).
- [15] P. J. Hay and W. R. Wadt, *J. Chem. Phys.* **82**, 299 (1985).
- [16] S. Huzinaga *et al.*, *Gaussian Basis Sets for Molecular Calculations* (Elsevier, New York, 1984).
- [17] H. X. Zhang and K. Balasubramanian, *J. Chem. Phys.* **97**, 3437 (1992).
- [18] J. A. Pople, R. Seeger, and R. Krishnan, *Int. J. Quantum Chem.* **11**, 149 (1977).
- [19] R. S. Mulliken, *J. Chem. Phys.* **36**, 3428 (1962).
- [20] P. Fantucci, J. Kautecky, and G. Pacchioni, *J. Chem. Phys.* **80**, 325 (1983).
- [21] A. Hartmann and K. G. Weil, *Z. Phys.* **12**, 11 (1989).
- [22] H. Lies, M. C. Böhm, and K. G. Weil, *Ber. Bunsenges. Phys. Chem.* (to be published).